Semnan University

Mechanics of Advanced Composite Structures

journal homepage: http://MACS.journals.semnan.ac.ir

Size-dependent Electro-Mechanical Vibration Analysis of FGPM Composite Plates using Modified Shear Deformation Theories

K. Khorshidi [a,b*], M. Karimi [a], A. Siahpush [a]

[a] *Department of Mechanical Engineering, Arak University, Arak, 38156-88349, Iran*
[b] *Institute of Nanosciences & Nanotechnolgy, Arak University, Arak, 38156-88349, Iran*

KEYWORDS

FGPM,
Electro-mechanical loads,
Free Vibration,
Nonlocal,
Modified shear deformation theory

ABSTRACT

In the current study, the modified shear deformation theories are used for analyzing the electro-mechanical vibration of inhomogeneous piezoelectric nanoplates in conjunction with the nonlocal elasticity theory. These theories not only satisfy transverse shear traction-free conditions on the top and bottom surfaces of the plate but also consider exponential and trigonometric distributions for the transverse shear deformations. Heterogeneity of the structure is supposed to be in the thickness direction of the nanoplate and it is assumed that the simply supported functionally graded piezoelectric nanoplate is subjected to a biaxial force and an external electric voltage. The governing equations of the vibrating functionally graded piezoelectric nanoplate are obtained by using Hamilton's principle, which are then solved by using Navier's method to achieve the vibrational behavior of the structure. The detailed discussion is presented to explain the influences of the various parameters on the natural frequencies of functionally graded piezoelectric nanoplates. It is concluded that increasing gradient index parameter, nonlocal parameter, thickness ratio and compressive forces lead to a decrease in natural frequencies while rising tensile forces and aspect ratio increase the natural frequencies.

1. Introduction

In the domain of material science, there are many smart or intelligent substances made by piezoelectric materials. Piezoelectric materials have been broadly utilized as components of sensors and actuators in control systems due to their electromechanical properties, allowing to convert electrical energy into mechanical energy and vice versa. With the trends toward device miniaturization, piezoelectric materials and their nanostructures have received much attention among researchers who are interested in both experimental and theoretical studies. Nano-sized structures, where thickness is routinely based on microns and sub-microns, have been substantially used in many devices and systems, such as microsensors, micro-actuators, nano/micro-electromechanical systems (NEMS and MEMS). The active vibration control of plates is one of researchers' favorite topics. Li et al. [1] investigated the vibration control of plates using piezoelectric patches. Khorshidi et al. [2] investigated the active vibration control of circular plates including piezoelectric layers under the plane sound wave excitation.

Conventional continuum models do not entail size effects due to the lack of material length scale parameters. Thus, there is a need for the development of size-dependent continuum models capturing size effects. In general, size-dependent models are based on nonclassical continuum theories such as the nonlocal elasticity theory [3], the couple stress theory [4], and the strain gradient theory [5]. In small scale structures, the influences of size are very evident and important, which has already been determined by many experiments and atomistic simulations [6, 7]. This is why the classical continuum model, which is a scale-independent theory, does not succeed to meet the computational requisites of nanostructures. Therefore, extensive high-order theories such as

* Corresponding author. Tel.: +98-86-32625720; Fax: +98-86-32625721
E-mail address: k-khorshidi@aaku.ac.ir

DOI: 10.22075/macs.2021.20177.1248
Received 2020-04-10; Received in revised form 2020-09-19; Accepted 2021-04-01

the nonlocal elasticity theory, the strain gradient theory, the couple stress theory and the micro-polar theory, are developed to modify the classical continuum model.

The nonlocal elasticity theory presented by Eringen [3] is usually implemented to evaluate the scale effect of nanostructures. This theory states that the stress of each point of the structure is dependent on the strains of all points in the body. This theory is applied to the nanoplates by imposing a length scale parameter into the constitutive equations as a material parameter. Meanwhile, different nonlocal and local models were developed to solve the buckling [8], linear and nonlinear vibrations of nanostructures such as graphene, carbon nanotubes, sheets, and etc. [9-13].

Additionally, the nonlocal theory has already been developed to examine the size-dependent mechanical behavior of the piezoelectric nanostructures [14-20]. Many mathematical and theoretical models have been presented for various structures with piezoelectric sensors and actuators. The main disadvantage of these structures is that the high stress concentrations commonly grow at the interface of layers subjected to the electro-mechanical forces. This weakness limits the suitability of piezoelectric devices in the application which the devices need high dependability. With regards to the low performance of the usual layered piezoelectric structures, the idea of functionally graded materials (FGMs) has been developed to the piezoelectric materials by modern advances in the metallurgical science and production techniques. In contrast to laminated composite materials, there are no interlaminar stresses for these materials as they vary continuously throughout the structure. The functionally graded piezoelectric materials, because of their immeasurable employment in many engineering fields, are used in various systems such as micro/nano electromechanical systems. Due to the steady change in the material contribution and properties from the bottom to the surface, this category of advanced materials is called functionally graded piezoelectric materials (FGPMs). The electric field and stress components depend on each other in the functionally graded piezoelectric materials. Also, their material properties continuously change in one (or more) direction(s). These attributes expand the intricacy and laboriousness of analyzing structures made of these materials. In recent years, the behaviors of functionally graded materials of plates have been studied extensively [21-29].

Plate deformation theories are separated into stress based and displacement-based theories. Displacement based theories can be divided into the classical plate theory and shear deformation plate theories. The use of shear deformation theories for composite and sandwich plates have been the subject of intense research. Transverse shear stress components in thickness direction are neglected in the classical theory of plates and this theory is used only for thin plates since it leads to inappropriate results for thick plates especially those made from advanced composites. Under the assumption of classical plate theory straight lines normal to the midplane before deformation, remain straight and normal to the midplane after deformation. The first order shear deformation theory is considered as an improvement over the classical plate theory. It is based on the supposition that straight lines normal to the midplane before deformation remain straight but, inevitably, not normal to the deformed midplane. First-order shear deformation theory incorporates the shear deformation effects with a constant transverse shear deformation distribution along the thickness of the plate. Thus, it violates stress-free conditions at the bottom and top of the plate and needs a shear correction factor to compensate this error. The limitations of the classical plate theory and the first order shear deformation theory resulted in the development of higher order shear deformation theories. Various distributions of transverse shear stress can be found in the literature for analyzing different structures [30-43]. In the exponential and trigonometric shear deformation theories, exponential and trigonometric functions are applied distribution.

The intent of this study is to investigate the free electro-mechanical vibration of functionally graded piezoelectric nanoplates using the nonlocal elasticity theory. The mechanical and electrical properties of the assumed structure are considered to change according to the power law through the thickness of the nanoplate, and the structure is imposed to the different loadings. After obtaining the vibration characteristics of the nanoplate using Navier's method, some comparison studies are provided to describe the reliability and efficacy of the present work. In the discussion section, the influences of the different parameters like nonlocal parameter, gradient index, biaxial forces, the external electrical force and the geometrical ratios on the electro-mechanical vibration characteristics of functionally graded piezoelectric nanoplates are shown.

2. Formulation of FGPMs

Consider a finite rectangular nanoplate made of functionally graded piezoelectric materials of length l_a, width l_b and thickness h, defined in the rectangular coordinate system ($0 \leq x \leq l_a$, $0 \leq$

$y \le l_b$, $-h/2 \le z \le h/2$). The nanoplate is subjected to a mechanical biaxial force P_0 (compressive force or tensile force) and an external electric voltage V_0 as shown in Fig. 1. The poling direction of the piezoelectric medium is parallel to the positive z-axis. The effective material properties of considered functionally graded piezoelectric nanoplate continuously vary through the thickness direction in accordance with the power law distribution as follows

$$\Pi = \Pi_u V_{u_{(z)}} + \Pi_l V_{l_{(z)}}, \quad (1)$$

where Π_u and v represent the material properties at the upper and lower surfaces, respectively, and $V_{u_{(z)}}$ and $V_{l_{(z)}}$ are the corresponding volume fractions defined as

$$V_{u_{(z)}} = \left(\frac{z}{h} + \frac{1}{2}\right)^{\lambda}, V_{l_{(z)}} = 1 - V_{u_{(z)}}, \quad (2)$$

And a gradient index λ $0 \le \lambda < \infty$ implies the variation of material properties across the nanoplate thickness.

2-1. Nonlocal theory for FGPMs

In order to consider length scale on mechanical behavior of piezoelectric nanoplates, nonlocal theory has been commonly utilized. According to the Eringen's nonlocal elasticity theory, stress at a point X in a body depends on strains of the whole domain [3]. By introducing a nonlocal attenuation function to consider for the effect of long-range interatomic forces, the nonlocal elasticity theory explains satisfactorily some phenomena such as the high frequency vibration and wave dispersion. Mathematically, neglecting the effect of body forces, the basic equations for a functionally graded and nonlocal piezoelectric solid can be expressed as [2, 3].

$$\sigma_{ij} = \int_{\Gamma} \alpha(|X' - X|, e_0 a/l) \left[C_{ijkl}\varepsilon_{kl}(X') - e_{kij}E_k(X')\right] dX', \quad \forall X \in \Gamma, \quad (3)$$

$$D_i = \int_{\Gamma} \alpha(|X' - X|, e_0 a/l) \left[e_{ikl}\varepsilon_{kl}(X') + d_{ki}E_k(X')\right] dX', \quad \forall X \in \Gamma, \quad (4)$$

$$\sigma_{ij,j} = \rho\ddot{u}_i \quad (5)$$

$$D_{i,i} = 0 \quad (6)$$

$$\varepsilon_{ij} = \frac{1}{2}\left(u_{i,j} + u_{j,i}\right) \quad (7)$$

$$E_i = -\Phi_i \quad (8)$$

where Γ is continuum occupying region, σ_{ij}, ε_{kl}, D_i and E_k are the components of the stress, strain, electric displacement and electric field, respectively. Also, C_{ijkl}, e_{ijk}, d_{ik} and ρ are the elastic, piezoelectric, dielectric coefficients and mass density, respectively, Φ is electric potential. $\alpha(|X' - X|, e_0 a/l)$ represents the nonlocal attenuation function, considering size effects at the reference point. e_0 is a calibration constant appropriate to each material.

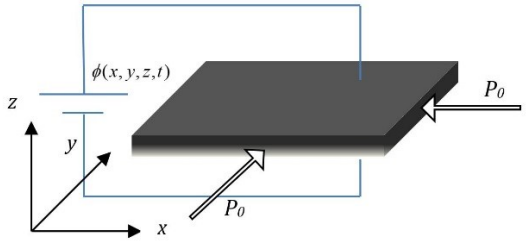

Fig. 1. Geometry and dimensions of the functionally graded piezoelectric nanoplate under eletro-mechenical loadings.

The measure of e_0 is determined experimentally or estimated such that the relations of the nonlocal elasticity model could provide satisfactory approximations to the atomic dispersion curves of the plane waves with those obtained from the atomistic lattice dynamics [44]. a and l are the internal (e.g. C–C bond length, granular distance, lattice parameter) and external (e.g. crack length, wavelength) characteristic lengths of the nanostructures, respectively. When the internal characteristic length is zero, nonlocal elasticity reduces to the classical (local) elasticity [45]. The constitutive equations for the functionally graded piezoelectric solids may be demonstrated with an equivalent differential form as,

$$(1 - (e_0 a)^2 \nabla^2)\sigma_{ij} = C_{ijkl}\varepsilon_{kl} - e_{ijk}E_k, \quad (9)$$

$$(1 - (e_0 a)^2 \nabla^2)D_i = e_{ikl}\varepsilon_{kl} + d_{ik}E_k, \quad (10)$$

where ∇^2 is the Laplace operator; $e_0 a$ is the scale coefficient revealing the size effect on the response of nanostructures. For the functionally graded piezoelectric structures, where thickness is much smaller than its length and width, the behavior of the structure can be estimated based on two-dimensional analysis. Therefore, for plates in the (x, y, z) coordinate system, ignoring the nonlocal behavior in the thickness direction, the nonlocal constitutive relations (9) and (10) can be approximated as,

$$(1 - (e_0 a)^2 \nabla^2)\begin{Bmatrix} \sigma_{xx} \\ \sigma_{yy} \\ \sigma_{xy} \\ \sigma_{xz} \\ \sigma_{yz} \end{Bmatrix} = \begin{bmatrix} \tilde{C}_{11} & \tilde{C}_{12} & 0 & 0 & 0 \\ \tilde{C}_{12} & \tilde{C}_{11} & 0 & 0 & 0 \\ 0 & 0 & \tilde{C}_{66} & 0 & 0 \\ 0 & 0 & 0 & \tilde{C}_{44} & 0 \\ 0 & 0 & 0 & 0 & \tilde{C}_{44} \end{bmatrix} \begin{Bmatrix} \varepsilon_{xx} \\ \varepsilon_{yy} \\ \gamma_{xy} \\ \gamma_{xz} \\ \gamma_{yz} \end{Bmatrix} - \begin{bmatrix} 0 & 0 & \tilde{e}_{31} \\ 0 & 0 & \tilde{e}_{31} \\ 0 & 0 & 0 \\ \tilde{e}_{15} & 0 & 0 \\ 0 & \tilde{e}_{15} & 0 \end{bmatrix} \begin{Bmatrix} E_x \\ E_y \\ E_z \end{Bmatrix}, \quad (11)$$

$$(1-(e_0a)^2\nabla^2)\begin{Bmatrix}D_x\\D_y\\D_z\end{Bmatrix}= \quad (12)$$
$$\begin{bmatrix}0&0&0&\tilde{e}_{15}&0\\0&0&0&0&\tilde{e}_{15}\\\tilde{e}_{31}&\tilde{e}_{31}&0&0&0\end{bmatrix}\begin{Bmatrix}\varepsilon_{xx}\\\varepsilon_{yy}\\\varepsilon_{xy}\\\varepsilon_{xz}\\\varepsilon_{yz}\end{Bmatrix}+$$
$$\begin{bmatrix}\tilde{d}_{11}&0&0\\0&\tilde{d}_{11}&0\\0&0&\tilde{d}_{33}\end{bmatrix}\begin{Bmatrix}E_x\\E_y\\E_z\end{Bmatrix},$$

where $\tilde{C}_{ij}$, $\tilde{e}_{ij}$ and $\tilde{d}_{ij}$ are respectively the reduced elasticity constants, piezoelectric constants and dielectric constants for the functionally graded piezoelectric nanoplate under the plane stress state [18]. These constants are defined as,

$$\tilde{C}_{11}=c_{11}-\frac{{c_{13}}^2}{c_{33}} \quad (13)$$
$$\tilde{C}_{12}=c_{12}-\frac{{c_{13}}^2}{c_{33}} \quad (14)$$
$$\tilde{C}_{44}=c_{44} \quad (15)$$
$$\tilde{e}_{31}=e_{31}-\frac{c_{13}e_{33}}{c_{33}} \quad (16)$$
$$\tilde{C}_{66}=c_{66} \quad (17)$$
$$\tilde{e}_{15}=e_{15} \quad (18)$$
$$\tilde{d}_{11}=d_{11} \quad (19)$$
$$\tilde{d}_{33}=d_{33}+\frac{{e_{33}}^2}{c_{33}} \quad (20)$$

where c_{ij}, e_{ij} and d_{ij} are respectively the elasticity constants, piezoelectric constants and dielectric constants.

2-2. Free vibration analysis of the FGPMs

Based on the exponential and trigonometric shear deformation theories, the displacement field of the functionally graded piezoelectric nanoplate is given as below [39],

$$u_1(x,y,z,t)=u(x,y,t)-z\frac{\partial w(x,y,t)}{\partial x}+f(z)\xi(x,y,t), \quad (21)$$
$$u_2(x,y,z,t)=v(x,y,t)-z\frac{\partial w(x,y,t)}{\partial y}+f(z)\psi(x,y,t), \quad (22)$$
$$u_3(x,y,z,t)=w(x,y,t), \quad (23)$$

where $u_1(x,y,z,t)$ and $u_2(x,y,z,t)$ are the in-plane displacements at any point (x,y,z), $u(x,y,t)$ and $v(x,y,t)$ denote displacement of the mid-plane and $w(x,y,t)$ is deflection of the functionally graded piezoelectric nanoplate in the x, y and z directions, respectively. Also $\xi(x,y,t)$ and $\psi(x,y,t)$ are rotations of the normals to the mid-plane about the y and x axes, respectively, additionally, $f(z)$ represents the distribution of the transverse shear strains and stresses along the thickness.

Time is expressed by t, and $f(z)$ for exponential and trigonometric shear deformation theories can be described as follows [20],

$$f(z)=ze^{-2\left(\frac{z}{h}\right)^2}, \quad (24)$$
$$f(z)=\frac{h}{\pi}\sin\left(\frac{\pi z}{h}\right). \quad (25)$$

The present nanoplate model should be assumed to satisfy the Maxwell equation [46]. The electric potential is approximately assumed as a combination of cosine and linear variation.

$$\widehat{\Phi}(x,y,z,t)=-\cos(\gamma z)\,\varphi(x,y,t)+\frac{2\,z\,V_0}{h}e^{i\,\Omega\,t}, \quad (26)$$

where $=\pi/h$, φ is the spatial and time variation of the electric potential in the mid-plane of the nanoplate, V_0 is the external electric voltage and Ω is the natural frequency of the functionally graded piezoelectric nanoplate. Hence the components of the linear strain tensor of the functionally graded piezoelectric nanoplate are

$$\varepsilon_{xx}=\frac{\partial u}{\partial x}-z\frac{\partial^2 w}{\partial x^2}+f_{(z)}\frac{\partial \xi}{\partial x}\ ,\quad \varepsilon_{yy}=\frac{\partial v}{\partial y}-z\frac{\partial^2 w}{\partial y^2}+f_{(z)}\frac{\partial \psi}{\partial y}, \quad (27,28)$$
$$\varepsilon_{xy}=\frac{1}{2}\left(\frac{\partial u}{\partial y}+\frac{\partial v}{\partial x}-2z\frac{\partial^2 w}{\partial x\partial y}+f_{(z)}\left(\frac{\partial \xi}{\partial y}+\frac{\partial \psi}{\partial x}\right)\right), \quad (29)$$
$$\varepsilon_{zz}=0,\quad \varepsilon_{xz}=\frac{1}{2}\frac{df_{(z)}}{dz}\xi,\quad \varepsilon_{yz}=\frac{1}{2}\frac{df_{(z)}}{dz}\psi. \quad (30\text{-}32)$$

Using Eq. (26), the electric fields can be expressed as,

$$E_x=-\frac{\partial\widehat{\Phi}}{\partial x}=\cos(\gamma z)\frac{\partial\varphi}{\partial x}, \quad (33)$$
$$E_y=-\frac{\partial\widehat{\Phi}}{\partial y}=\cos(\gamma z)\frac{\partial\varphi}{\partial y}, \quad (34)$$
$$E_z=-\frac{\partial\widehat{\Phi}}{\partial z}=-\gamma\sin(\gamma z)\,\varphi-\frac{2V_0}{h}e^{i\Omega t}. \quad (35)$$

Then, the strain energy U of the piezoelectric nanoplate is given by

$$U=\frac{1}{2}\int_\Gamma\left(\sigma_{xx}\varepsilon_{xx}+\sigma_{yy}\varepsilon_{yy}+2\sigma_{xy}\varepsilon_{xy}+2\sigma_{xz}\varepsilon_{xz}+2\sigma_{yz}\varepsilon_{yz}-D_xE_x-D_yE_y-D_zE_z\right)d\Gamma. \quad (36)$$

The first variation of strain energy can be written as,

$$\delta U=\int_\Gamma\left(-\frac{\partial^2 M_x}{\partial x^2}\delta w-2\frac{\partial^2 M_{xy}}{\partial x\partial y}\delta w-\frac{\partial^2 M_y}{\partial y^2}\delta w-\frac{\partial N_x}{\partial x}\delta u-\frac{\partial N_{xy}}{\partial x}\delta v-\frac{\partial N_{xy}}{\partial y}\delta u-\frac{\partial N_y}{\partial y}\delta v-\frac{\partial P_x}{\partial x}\delta\xi-\frac{\partial P_{xy}}{\partial x}\delta\psi-\frac{\partial P_{xy}}{\partial y}\delta\xi-\frac{\partial P_y}{\partial y}\delta\psi+Q_{xz}\delta\xi+Q_{yz}\delta\psi+\frac{\partial D_x}{\partial x}\cos(\gamma z)\,\delta\varphi+\frac{\partial D_y}{\partial y}\cos(\gamma z)\,\delta\varphi+D_z\gamma\sin(\gamma z)\,\delta\varphi\right)d\Gamma, \quad (37)$$

where the resultant forces (N_x, N_y), (P_x,P_y,P_{xy}) and (Q_{xz},Q_{yz}), bending moment M_x, M_y and twisting moment M_{xy} can be written as follows,

$$\{N_x, N_y, N_{xy}\} = \int_{-h/2}^{h/2}\{\sigma_x, \sigma_y, \sigma_{xy}\}dz, \quad (38)$$

$$\{P_x, P_y, P_{xy}\} = \int_{-h/2}^{h/2}\{\sigma_x, \sigma_y, \sigma_{xy}\}f_{(z)}dz, \quad (39)$$

$$\{Q_{xz}, Q_{yz}\} = \int_{-h/2}^{h/2}\{\sigma_{xz}, \sigma_{yz}\}\frac{df_{(z)}}{dz}dz, \quad (40)$$

$$\{M_x, M_y, M_{xy}\} = \int_{-h/2}^{h/2}\{\sigma_x, \sigma_y, \sigma_{xy}\}zdz. \quad (41)$$

The kinetic energy T can be calculated as,

$$T = \frac{1}{2}\int_{\Gamma}\rho\left(\dot{u}_1{}^2 + \dot{u}_2{}^2 + \dot{u}_3{}^2\right)d\Gamma, \quad (42)$$

where dot-over script convention indicates the differentiation with respect to the time variable t. From Eqs. (12-14) and (28), the first variation of the kinetic energy can be expressed as,

$$\begin{aligned}\delta T = \int_{\Gamma}\Big(&-\frac{\partial^2\psi}{\partial t^2}I_4\delta v - \frac{\partial^2\psi}{\partial t^2}I_6\delta\psi - \frac{\partial^2\xi}{\partial t^2}I_4\delta u - \frac{\partial^2\xi}{\partial t^2}I_6\delta\xi - \frac{\partial^3\xi}{\partial t^2\partial x}I_5\delta w - \\ &\frac{\partial^2 u}{\partial t^2}I_1\delta u\ \frac{\partial^2 v}{\partial t^2}I_1\delta v - \frac{\partial^2}{\partial t^2}I_1\delta w - \frac{\partial^3 u}{\partial t^2\partial x}I_2\delta w - \frac{\partial^3 v}{\partial t^2\partial y}I_2\delta w + \frac{\partial^3}{\partial}I_2\delta u + \\ &\frac{\partial^3 w}{\partial t^2\partial y}I_2\delta v + \frac{\partial^4 w}{\partial t^2\partial x^2}I_3\delta w + \frac{\partial^4 w}{\partial t^2\partial y^2}I_3\delta w - \frac{\partial^2 u}{\partial t^2}I_4\delta\xi - \frac{\partial^2 v}{\partial t^2}I_4\delta\psi + \\ &\frac{\partial^3 w}{\partial t^2\partial x}I_5\delta\xi + \frac{\partial^3 w}{\partial t^2\partial y}I_5\delta\psi - \frac{\partial^3\psi}{\partial t^2\partial y}I_5\delta w\Big)d\Gamma,\end{aligned} \quad (43)$$

where inertia coefficients can be expressed as,

$$(I_1, I_2, I_3, I_4, I_5, I_6) = \int_{-h/2}^{h/2}\rho\left(1, z, z^2, f_{(z)}, zf_{(z)}, f_{(z)}{}^2\right). \quad (44)$$

The work done by external forces is denoted by W_f

$$W_f = \frac{1}{2}\int_A\left[(F_{Px} + F_{Ex})\left(\frac{\partial w}{\partial x}\right)^2 + \left(F_{Py} + F_{Ey}\right)\left(\frac{\partial w}{\partial y}\right)^2\right]dA, \quad (45)$$

where A denotes the domain occupied by the mid-plane of the functionally graded piezoelectric nanoplate and (F_{Px}, F_{Py}) and (F_{Ex}, F_{Ey}) are the normal forces induced by the biaxial force P_0, external electric voltage V_0 along the x- and y-axis. Moreover, $e_{31_{av.}}$ is average value of $\tilde{e}_{31}$ along the thickness which can be written as,

$$F_{Px} = F_{Py} = P_0, \quad (46)$$

$$F_{Ex} = F_{Ey} = -2e_{31_{av.}}V_0. \quad (47)$$

Herein, Hamilton's principle is used to derive equations of motion based on the modified shear deformation theories. The principle in case of local form can be stated as follows,

$$\int_0^t\left(\delta T + \delta W_f - \delta U\right)dt = 0, \quad (48)$$

By substituting Eqs. (37, 43 and 45) in the expression (48) of the principle of virtual works, integrating it by parts and setting the coefficients of $\delta u, \delta v, \delta w, \delta\xi, \delta\psi$ and $\delta\varphi$ to zero, the governing equations of motion for a functionally graded piezoelectric nanoplate are derived as,

$$-\frac{\partial^2\xi}{\partial t^2}I_4 - \frac{\partial^2 u}{\partial t^2}I_1 + \frac{\partial^3 w}{\partial t^2\partial x}I_2 + \frac{\partial N_x}{\partial x} + \frac{\partial N_{xy}}{\partial y} = 0, \quad (49)$$

$$-\frac{\partial^2\psi}{\partial t^2}I_4 - \frac{\partial^2 v}{\partial t^2}I_1 + \frac{\partial^3 w}{\partial t^2\partial y}I_2 + \frac{\partial N_y}{\partial y} + \frac{\partial N_{xy}}{\partial x} = 0, \quad (50)$$

$$\begin{aligned}&-\frac{\partial^3\xi}{\partial t^2\partial x}I_5 - \frac{\partial^2 w}{\partial x^2}F_x - \frac{\partial^2 w}{\partial y^2}F_y - \frac{\partial^2 w}{\partial t^2}I_1 - \frac{\partial^3 u}{\partial t^2\partial x}I_2 - \frac{\partial^3 v}{\partial t^2\partial y}I_2 + \\ &\frac{\partial^4 w}{\partial t^2\partial x^2}I_3 + \frac{\partial^4 w}{\partial t^2\partial y^2}I_3 - \frac{\partial^3\psi}{\partial t^2\partial y}I_5 + \frac{\partial^2 M_x}{\partial x^2} + 2\frac{\partial^2 M_{xy}}{\partial x\partial y} + \frac{\partial^2 M_y}{\partial y^2} = 0,\end{aligned} \quad (51)$$

$$-\frac{\partial^2\xi}{\partial t^2}I_6 - \frac{\partial^2 u}{\partial t^2}I_4 + \frac{\partial^3 w}{\partial t^2\partial x}I_5 + \frac{\partial P_x}{\partial x} + \frac{\partial P_{xy}}{\partial y} - Q_{xz} = 0, \quad (52)$$

$$-\frac{\partial^2\psi}{\partial t^2}I_6 - \frac{\partial^2 v}{\partial t^2}I_4 + \frac{\partial^3 w}{\partial t^2\partial y}I_5 + \frac{\partial P_y}{\partial y} + \frac{\partial P_{xy}}{\partial x} - Q_{yz} = 0, \quad (53)$$

$$-D_z\gamma\sin(\gamma z) - \frac{\partial D_x}{\partial x}\cos(\gamma z) - \frac{\partial D_y}{\partial y}\cos(\gamma z) = 0. \quad (54)$$

It is assumed that the functionally graded piezoelectric nanoplate has simply supported boundary conditions on all four edges and its edges are covered with electrodes and electrically grounded to zero potential. These mechanical and electrical boundary conditions can be written as follows,

$$u = 0 \quad \text{or} \quad N_x n_x + N_{xy} n_y = 0, \quad (55)$$

$$v = 0 \quad \text{or} \quad N_y n_y + N_{xy} n_x = 0, \quad (56)$$

$$w = 0 \quad \text{or} \quad n_x\left(\frac{\partial M_x}{\partial x} + (F_{px} + F_{Ex})\frac{\partial w}{\partial x}\right) + n_y\left(\frac{\partial M_y}{\partial y} + \frac{\partial M_{xy}}{\partial x} + (F_{py} + F_{Ey})\frac{\partial w}{\partial y}\right) = 0, \quad (57)$$

$$\frac{\partial w}{\partial x} = 0 \quad \text{or} \quad M_x n_x + M_y n_y = 0, \quad (58)$$

$$\frac{\partial w}{\partial y} = 0 \quad \text{or} \quad M_{xy} n_x = 0, \quad (59)$$

$$\xi = 0 \quad \text{or} \quad P_x n_x + M_{xy} n_y = 0, \quad (60)$$

$$\psi = 0 \quad \text{or} \quad P_y n_y + M_{xy} n_x = 0, \quad (61)$$

$$\varphi = 0 \quad \text{or} \quad \int_{-h/2}^{h/2}\cos(\gamma z)\, D_x n_x + \cos(\gamma z)\, D_y n_y = 0, \quad (62)$$

where (n_x, n_y) denote the direction cosines of the outward unit normal to the boundary of the mid-plane. By employing Eqs. (21, 23) on Eqs. (49-54) the nonlocal governing equations can be rewritten as,

$$\frac{\partial N_x}{\partial x} + \frac{\partial N_{xy}}{\partial y} = (1 - (e_0 a)^2\nabla^2)\left(-\frac{\partial^2\xi}{\partial t^2}I_4 - \frac{\partial^2 u}{\partial t^2}I_1 + \frac{\partial^3 w}{\partial t^2\partial x}I_2\right), \quad (63)$$

$$\frac{\partial N_y}{\partial y}+\frac{\partial N_{xy}}{\partial x}=(1-(e_0a)^2\nabla^2)\left(-\frac{\partial^2\psi}{\partial t^2}I_4-\frac{\partial^2 v}{\partial t^2}I_1+\frac{\partial^3 w}{\partial t^2\partial y}I_2\right), \quad (64)$$

$$\frac{\partial^2 M_x}{\partial x^2}+2\frac{\partial^2 M_{xy}}{\partial x\partial y}+\frac{\partial^2 M_y}{\partial y^2}=(1-(e_0a)^2\nabla^2)\left(-\frac{\partial^3\xi}{\partial t^2\partial x}I_5-\frac{\partial^2 w}{\partial x^2}F_x-\frac{\partial^2 w}{\partial y^2}F_y-\frac{\partial^2 w}{\partial t^2}I_1-\frac{\partial^3 u}{\partial t^2\partial x}I_2-\frac{\partial^3 v}{\partial t^2\partial y}I_2+\frac{\partial^4 w}{\partial t^2\partial x^2}I_3+\frac{\partial^4 w}{\partial t^2\partial y^2}I_3-\frac{\partial^3\psi}{\partial t^2\partial y}I_5\right), \quad (65)$$

$$\frac{\partial P_x}{\partial x}+\frac{\partial P_{xy}}{\partial y}-Q_{xz}=(1-(e_0a)^2\nabla^2)\left(-\frac{\partial^2\xi}{\partial t^2}I_6-\frac{\partial^2 u}{\partial t^2}I_4+\frac{\partial^3 w}{\partial t^2\partial x}I_5\right), \quad (66)$$

$$\frac{\partial P_y}{\partial y}+\frac{\partial P_{xy}}{\partial x}-Q_{yz}=(1-(e_0a)^2\nabla^2)\left(-\frac{\partial^2\psi}{\partial t^2}I_6-\frac{\partial^2 v}{\partial t^2}I_4+\frac{\partial^3 w}{\partial t^2\partial y}I_5\right), \quad (67)$$

$$-D_z\gamma\sin(\gamma z)-\frac{\partial D_x}{\partial x}\cos(\gamma z)-\frac{\partial D_y}{\partial y}\cos(\gamma z)=0. \quad (68)$$

Solution for the Eqs. (63-68) with aforementioned boundary conditions are assumed as following double Fourier series forms

$$\begin{Bmatrix}u\\v\\w\\\xi\\\psi\\\varphi\end{Bmatrix}=\sum_{m=1}^{\infty}\sum_{n=1}^{\infty}\begin{Bmatrix}U_{mn}\cos(\alpha x)\sin(\beta y)\\V_{mn}\sin(\alpha x)\cos(\beta y)\\W_{mn}\sin(\alpha x)\sin(\beta y)\\\Xi_{mn}\cos(\alpha x)\sin(\beta y)\\\Psi_{mn}\sin(\alpha x)\cos(\beta y)\\\Phi_{mn}\sin(\alpha x)\sin(\beta y)\end{Bmatrix}e^{i\Omega t} \quad (69)$$

where $\alpha=m\pi/l_a$, $\beta=n\pi/l_b$, and m and n denote the number of half waves in the x and y directions, respectively. U_{mn} , V_{mn} , W_{mn} , Ξ_{mn} , Ψ_{mn} and Φ_{mn} are Fourier coefficients to be determined for each (m,n). Clearly, the expansions in Eq. (69) exactly satisfy the boundary conditions in Eqs. (55-62) for any U_{mn} , V_{mn} , W_{mn} , Ξ_{mn} , Ψ_{mn} and Φ_{mn}. Substituting Eqs. (69) into Eqs. (63-68) yields

$$-A_1U_{mn}\alpha^2+A_2W_{mn}\alpha^3-A_4V_{mn}\alpha\beta-A_7V_{mn}\alpha\beta-A_7U_{mn}\beta^2+A_5W_{mn}\alpha\beta^2+2A_8W_{mn}\alpha\beta^2-A_3\xi_{mn}\alpha^2-A_9\Xi_{mn}\beta^2+B_1\Phi_{mn}\alpha-A_6\Psi_{mn}\alpha\beta-A_9\Psi_{mn}\alpha\beta+(1+(\alpha^2+\beta^2)e_0a)(I_1U_{mn}-I_2W_{mn}\alpha+I_4\Xi_{mn})\Omega^2=0, \quad (70)$$

$$-A_4U_{mn}\alpha\beta+A_5W_{mn}\alpha^2\beta+2A_8W_{mn}\alpha^2\beta-A_1V_{mn}\beta^2+A_2W_{mn}\beta^3-A_7\alpha(V_{mn}\alpha+U_{mn}\beta)-A_6\Xi_{mn}\alpha\beta-A_9\Xi_{mn}\alpha\beta+B_1\Phi_{mn}\beta-A_9\Psi_{mn}\alpha^2-A_3\Psi_{mn}\beta^2+(1+(\alpha^2+\beta^2)e_0a)(I_1V_{mn}-I_2W_{mn}\beta+I_4\Psi_{mn})\Omega^2=0, \quad (71)$$

$$(F_{px}+F_{Ex})W_{mn}\alpha^2+A_2U_{mn}\alpha^3-A_{10}W_{mn}\alpha^4+A_5V_{mn}\alpha^2\beta+2A_8V_{mn}\alpha^2\beta+(F_{py}+F_{Ey})W_{mn}\beta^2+A_5U_{mn}\alpha\beta^2+2A_8U_{mn}\alpha\beta^2-2A_{12}W_{mn}\alpha^2\beta^2-4A_{14}W_{mn}\alpha^2\beta^2+A_2V_{mn}\beta^3-A_{10}W_{mn}\beta^4+A_{11}\Xi_{mn}\alpha^3+A_{13}\alpha\beta^2\Xi_{mn}+2A_{15}\Xi_{mn}\alpha\beta^2-B_3\Phi_{mn}\alpha^2-B_3\Phi_{mn}\beta^2+A_{13}\Psi_{mn}\alpha^2\beta+2A_{15}\alpha^2\beta\Psi_{mn}+A_{11}\beta^3\Psi_{mn}+(1+(\alpha^2+\beta^2)e_0a)\big(I_1W_{mn}-I_2(U_{mn}\alpha+V_{mn}\beta)+I_3W_{mn}(\alpha^2+\beta^2)-I_5(\alpha\Xi_{mn}+\beta\Psi_{mn})\big)\Omega^2=0, \quad (72)$$

$$-A_3U_{mn}\alpha^2+A_{11}W_{mn}\alpha^3-A_6V_{mn}\alpha\beta-A_9V_{mn}\alpha\beta-A_9U_{mn}\beta^2+A_{13}W_{mn}\alpha\beta^2+2A_{15}W_{mn}\alpha\beta^2-A_{19}\Xi_{mn}-A_{16}\Xi_{mn}\alpha^2-A_{18}\Xi_{mn}\beta^2+B_5\Phi_{mn}\alpha+B_7\Phi_{mn}\alpha-A_{17}\Psi_{mn}\alpha\beta-A_{18}\Psi_{mn}\alpha\beta+(1+(\alpha^2+\beta^2)e_0a)(I_4U_{mn}-I_5W_{mn}\alpha+I_6\Xi_{mn})\Omega^2=0, \quad (73)$$

$$-A_6U_{mn}\alpha\beta+A_{13}W_{mn}\alpha^2\beta+2A_{15}W_{mn}\alpha^2\beta-A_3V_{mn}\beta^2+A_{11}W_{mn}\beta^3-A_9\alpha(V_{mn}\alpha+U_{mn}\beta)-A_{17}\alpha\beta\Xi_{mn}-A_{18}\Xi_{mn}\alpha\beta+B_5\beta\Phi_{mn}+B_7\Phi_{mn}\beta-A_{19}\Psi_{mn}-A_{18}\Psi_{mn}\alpha^2-A_{16}\Psi_{mn}\beta^2+(1+(\alpha^2+\beta^2)e_0a)(I_4V_{mn}-I_5W_{mn}\beta+I_6\Psi_{mn})\Omega^2, \quad (74)$$

$$B_1(U_{mn}\alpha+V_{mn}\beta)-B_3W_{mn}(\alpha^2+\beta^2)+B_5\Xi_{mn}\alpha+B_7\alpha\Xi_{mn}+B_9\varphi_{mn}+B_8\alpha^2\Phi_{mn}+B_8\beta^2\Phi_{mn}+(B_5+B_7)\beta\Psi_{mn}=0, \quad (75)$$

where A_i and B_j can be find in Appendix A. After simplification of the obtained equations, system of equations can be expressed as following matrix form,

$$[\tilde{K}]\{Y\}-[\tilde{M}]\{\ddot{Y}\}=0, \quad (76)$$

where the vector $\{Y\}$ is

$$\{Y\}=\{U_{mn}\quad V_{mn}\quad W_{mn}\quad \Xi_{mn}\quad \Psi_{mn}\quad \Phi_{mn}\} \quad (77)$$

Also $[\tilde{K}]$ and $[\tilde{M}]$ are stiffness and mass matrix respectively. This matrix eigenvalue problem should be solved to obtain the natural frequencies of functionally graded piezoelectric nanoplate [20].

3. Results and discussion

This section will present the numerical results for the electro-mechanical vibration of the functionally graded piezoelectric nanoplate under simply supported boundary conditions. The functionally graded piezoelectric nanoplate made of PZT-4 and PZT-5H piezoelectric

materials are the subject of analysis. The top surface of the nanoplate is PZT-4 rich, while the bottom one is PZT-5H rich. Table 1 represents the electro-mechanical properties of these constituents [47]. In addition, it is assumed that the length of the functionally graded piezoelectric nanoplate is $l_a = 50$ nm, the width of the nanoplate is $l_b = 35$ nm and thickness is $h = 5$ nm. The effects of various values of the dimensionless nonlocal parameter ($\mu = \frac{e_0 a}{l_a}$), gradient index λ, biaxial force P_0, external electric potential V_0, aspect ratio l_a/l_b and side-to-thickness ratio l_a/h on the dimensionless natural frequencies$\left(\omega = \Omega h\sqrt{(\rho/c_{11})_{PZT-5H}}\right)$ of the functionally graded piezoelectric nanoplates were investigated and discussed in details.

To check the validity and accuracy of the present analysis, the results obtained from the present analysis are compared with those available in the literature for functionally graded piezoelectric square plates, and also for homogeneous piezoelectric nanoplates ($\lambda = 0$). Bodaghi and Shakeri [47] analyzed the free vibration of functionally graded cylindrical panels based on the nonlocal theory of elasticity using the analytical method. And the free vibration analysis of nonlocal homogeneous piezoelectric nanoplates was presented by Ke et al. based on Mindlin's theory using the Differential quadrature (DQ) method [18] and also Liu et al. analyzed the free vibration of piezoelectric nanoplates based on the Kirchhoff's theory with the analytical method [17]. Therefore, this sub-section will present two examples for the nonlocal elastic nanoplates to ensure the validity of the present model. In Table 2 the dimensionless fundamental frequencies $\left(\omega = \Omega l_a\sqrt{(\rho/c_{11})_{PZT4}}\right)$ of simply supported homogeneous piezoelectric nanoplates calculated by the present method are compared with those reported by Liu et al. [17] and Ke et al. [18].

It is observed that the results obtained on the basis of the present method have good agreement with the available data. The parameters used in this example are $l_a = l_b = 50$ nm, $h = 5$ nm, $\lambda = 0$, $P_0 = 0$ and $V_0 = 0$. It can be said that the effect of shear deformation is significant for small thickness-to-length ratios and it diminishes with an increase in length-to-thickness ratio. As a second example, Table 3 depicts the dimensionless natural frequencies $\left(\omega = \Omega h\sqrt{(\rho/c_{11})_{PZT-5H}}\right)$ of the functionally graded piezoelectric nanoplate for different gradient index values. In this reference, material properties of the functionally graded piezoelectric plate vary from PZT-4 to PZT-5H according to the power law function.

The input parameters are $l_a = l_b = 50\,nm$, $h = 5\,nm$, $\mu = 0$, $P_0 = 0$ and $V_0 = 0$ and the piezoelectric plate has been analyzed with the exponential shear deformation theory. And again, the present results agree well with the Mindlin's plate theory.

The difference of the results is due to the difference between distributions of transverse shear deformation and rotation effects in modified shear deformation theories. Moreover, modified shear deformation theories do not require any shear correction factor and satisfy transverse shear traction-free conditions on the top and bottom surfaces of the nanoplate. The effect of the nonlocal parameter μ on the first six dimensionless natural frequencies of the functionally graded piezoelectric nanoplate with $P_0 = 0$, $V_0 = 0$ and $\lambda = 1$ is listed in the Table 4. Note that the nonlocal parameter $\mu = 0$ corresponds to the classical piezoelectric nanoplate model without considering the nonlocal effect. It can be observed that the dimensionless natural frequencies predicted by the present model tend to be smaller than those of the classical model. The nonlocal parameter μ has an important influence on natural frequencies and increasing nonlocal parameter decreases the natural frequencies. This phenomenon is caused by nonlocal effect, which considers the conjoint effect of all points in the domain, and it decreases the stiffness of the nanostructures and as a result drops the values of the natural frequencies.

As seen in Table 5, the dimensionless natural frequency parameter has experienced a decline by increasing of the gradient index of functionally graded piezoelectric nanoplate which is due to the changing of material properties from PZT-4 to PZT-5H.

Table 1. Material properties of the PZT-4 and the PZT-5H [47].

Parameters	PZT-4	PZT-5H
C_{11}(GPa)	139	126
C_{13}(GPa)	74	83.9
C_{33}(GPa)	115	117
C_{12}(GPa)	77.8	79.1
C_{13}(GPa)	74	83.9
C_{44}(GPa)	25.6	23
C_{66}(GPa)	30.6	23.5
e_{31}(C/m^2)	-5.2	-6.5
e_{33}(C/m^2)	15.1	23.3
e_{15}(C/m^2)	12.7	17
d_{11}(nF/m)	6.46	15.05
d_{33}(nF/m)	5.62	13.02
ρ(Kg/m^3)	7500	7500

Table 2. Comparison of dimensionless natural frequency for piezoelectric nanoplate under different distributions of transverse shear deformation.

μ	$\frac{l_a}{h}=10$				$\frac{l_a}{h}=40$			
	Exp.	Tri.	CPT [17]	FSDT [18]	Exp.	Tri.	CPT [17]	FSDT [18]
0	064	0.6059	0.6290	0.6068	0.1568	0.1566	0.1574	0.1570
0.1	0.5541	0.5535	0.5748	0.5545	0.1432	0.1429	0.1439	0.1435
0.2	0.4533	0.4529	0.4702	0.4536	0.1171	0.1168	0.1177	0.1174
0.3	0.3637	0.3634	0.3775	0.3641	0.0940	0.0937	0.0945	0.0943
0.4	0.2972	0.2967	0.3085	0.2976	0.0768	0.0764	0.0772	0.0770
0.5	0.2489	0.2487	0.2582	0.2491	0.0642	0.0638	0.0646	0.0645

Table 3. Comparison of the dimensionless fundamental frequency for the simply supported functionally graded piezoelectric square plate using the exponential shear deformation theory.

$\frac{l_a}{h}$		λ				
		0	1	3	5	10
20	Exp.	0.01378	0.01300	0.01277	0.01269	0.01257
	FSDT [23]	0.01380	0.01301	0.01290	0.01285	0.01279
10	Exp.	0.05363	0.05063	0.04979	0.04946	0.04901
	FSDT [23]	0.05365	0.05065	0.05025	0.05008	0.04985

Table 4. The effect of the nonlocal parameter μ on the dimensionless natural frequencies of functionally graded piezoelectric nanoplate.

		μ					
		0	0.1	0.2	0.3	0.4	0.5
ω_1	Exp.	0.07336	0.06434	0.04945	0.03813	0.03046	0.02516
	Tri.	0.07335	0.06433	0.04944	0.03811	0.03045	0.02515
ω_2	Exp.	0.13944	0.11037	0.07579	0.05527	0.04295	0.03496
	Tri.	0.13940	0.11033	0.07577	0.05525	0.04294	0.03495
ω_3	Exp.	0.20308	0.14716	0.09451	0.06718	0.05163	0.04180
	Tri.	0.20300	0.14710	0.09447	0.06715	0.05161	0.04178
ω_4	Exp.	0.23930	0.16554	0.10337	0.07279	0.05573	0.04503
	Tri.	0.23918	0.16546	0.10332	0.07276	0.05571	0.04501
ω_5	Exp.	0.26031	0.17548	0.10807	0.07576	0.05791	0.04674
	Tri.	0.26017	0.17539	0.10801	0.07572	0.05788	0.04672
ω_6	Exp.	0.34881	0.21252	0.12509	0.08654	0.06580	0.05298
	Tri.	0.34857	0.21237	0.12500	0.08648	0.06575	0.05294

In Fig. 2, the effects of the aspect ratio $\frac{l_a}{l_b}$ and the nonlocal parameter with $P_0 = 0$, $V_0 = 0$ and $\lambda = 1$ on the nondimensional fundamental frequency of the piezoelectric nanoplates using the exponential shear deformation theory are shown. Thickness value of the piezoelectric nanoplate is taken to be h=5 nm. The depicted results reveal that the dimensionless fundamental natural frequency first increases mildly when the aspect ratio varies from 0.2 to1.0 and then swiftly increases when the aspect ratio changes from 1.0 to 3.0. Also, the size effect on the piezoelectric nanoplate has an increasingly strong trend with the increase of the aspect ratio.

The effect of the length-to-thickness ratio $\frac{l_a}{h}$ on the first dimensionless natural frequency ω_1 of piezoelectric nanoplates is shown in Fig. 3 with $P_0 = 0$, $V_0 = 0$, $\mu = 0.4$ and $\lambda = 1$. It is observed that the dimensionless fundamental natural frequency reduces quickly with the raise of the length-to-thickness ratio. That is to say, the fundamental frequency for thick and relatively thick nanoplates is higher than thin nanoplates. Furthermore, Fig. 3 illustrates that when length-to-thickness ratio increases, the importance of the size effect reduces.

Figs. 4-5 examine the effect of different amounts of the biaxial force $P_0(N)$ on the first six dimensionless natural frequencies of the piezoelectric nanoplate with $\lambda = 1$, $\mu = 0.4$ and $V_0 = 0$. The positive and negative values of the biaxial forces signify the compressive force and tensile force, respectively.

Table 5. The effect of the gradient index λ on the dimensionless natural frequencies of functionally graded piezoelectric nanoplates.

		λ					
		0	0.3	1	5	10	∞
ω_1	Exp.	0.03768	0.03073	0.04046	0.03020	0.03009	0.02987
	Tri.	0.03767	0.03070	0.03044	0.03019	0.03007	0.02985
ω_2	Exp.	0.05306	0.04331	0.04295	0.04263	0.04249	0.04219
	Tri.	0.05304	0.04330	0.04294	0.04262	0.04248	0.04218
ω_3	Exp.	0.06371	0.05203	0.05163	0.05128	0.05113	0.05079
	Tri.	0.06368	0.05201	0.05161	0.05126	0.05111	0.05077
ω_4	Exp.	0.06872	0.05614	0.05573	0.05538	0.05522	0.05486
	Tri.	0.06869	0.05611	0.05571	0.05535	0.05519	0.05484
ω_5	Exp.	0.07138	0.05832	0.05791	0.05755	0.05739	0.05702
	Tri.	0.07134	0.05829	0.05788	0.05752	0.05736	0.05700
ω_6	Exp.	0.08101	0.06622	0.06580	0.06546	0.06528	0.06489
	Tri.	0.08095	0.06617	0.06575	0.06541	0.06524	0.06485

Clearly, when the stronger biaxial tensile force ($P_0 < 0$) is applied, the natural frequencies increase to higher values, and the reverse trend will occur for the biaxial compressive force($P_0 > 0$). The explanation is that compressive force weakens but tensile force strengthens the stiffness of piezoelectric nanoplates.

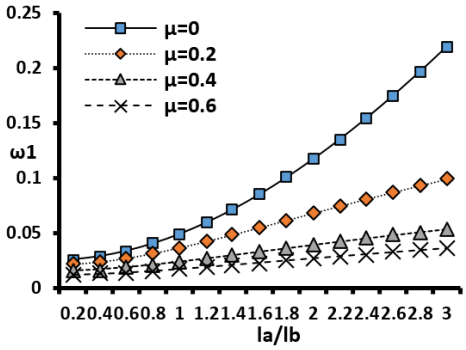

Fig. 2. The effects of the aspect ratio $\frac{l_a}{l_b}$ and nonlocal parameter μ on the dimensionless fundamental frequency ω_1 of functionally graded piezoelectric nanoplate with $P_0 = 0, V_0 = 0$ and $\lambda = 1$.

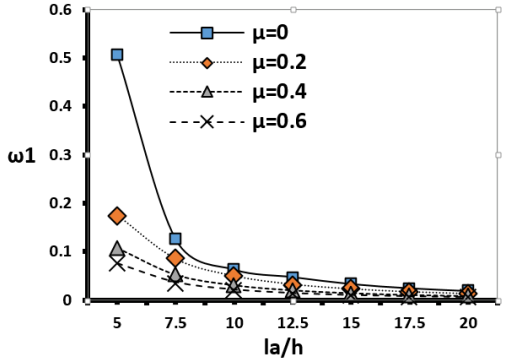

Fig. 3. The effect of the length-to-thickness ratio $\frac{l_a}{h}$ on the dimensionless fundamental frequency ω_1 of functionally graded piezoelectric nanoplate.

The effect of the external electric voltage $V_0(V)$ on the first six dimensionless natural frequencies of piezoelectric nanoplates with $\lambda = 1$, $\mu = 0.4$ and $P_0 = 0$ under exponential and trigonometric distributions of transverse shear deformation is described in Figs. 6-7, respectively.

It is found that the natural frequencies of the piezoelectric nanoplates are utterly dependent on the variation of the external electric voltage. So that the negative voltage heightens the natural frequencies of the piezoelectric nanoplates, while the positive voltage causes the contrary effect.

This is due to the fact that the axial compressive and tensile forces are generated in the nanostructure nanoplate by applying the positive and negative voltages, respectively. The tensile forces raise the stiffness value of the piezoelectric nanoplate structure, and therefore lead to the greater value of the natural frequencies while the compressive ones have the opposite reaction.

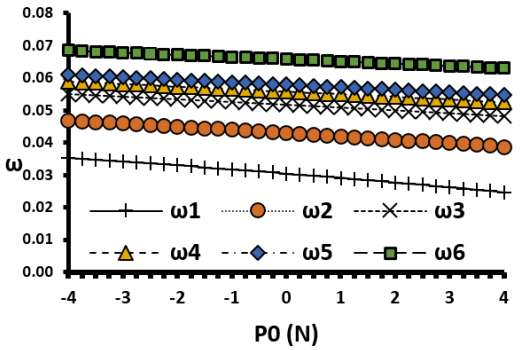

Fig. 4. The effect of the biaxial force P_0(N) on the dimensionless natural frequencies of the functionally graded piezoelectric nanoplate using exponential shear deformation theory with $\lambda = 1$, $\mu = 0.4$ and $V_0 = 0$.

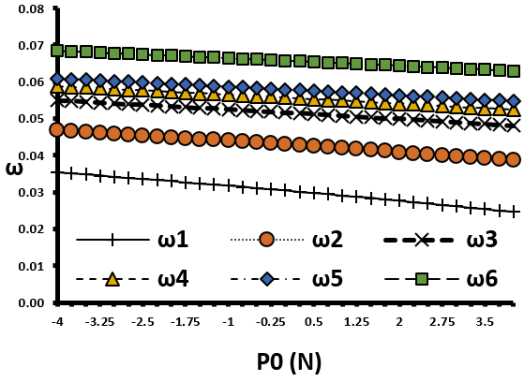

Fig 5. The effect of the biaxial force P_0(N) on the dimensionless natural frequencies of the functionally graded piezoelectric nanoplate using trigonometric shear deformation theory with $\lambda = 1$, $\mu = 0.4$ and $V_0 = 0$.

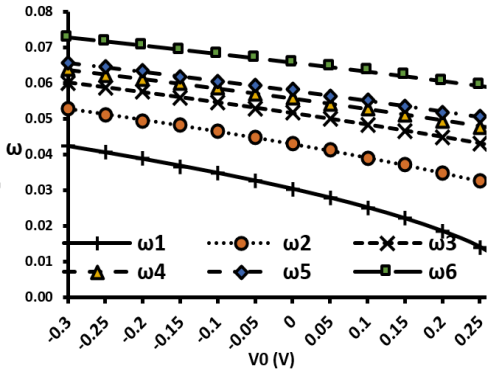

Fig. 6. The effect of the biaxial force V_0(V) on the dimensionless natural frequencies of the functionally graded piezoelectric nanoplate under exponential distribution of transverse shear deformation with $\lambda = 1$, $\mu = 0.4$ and $P_0 = 0$.

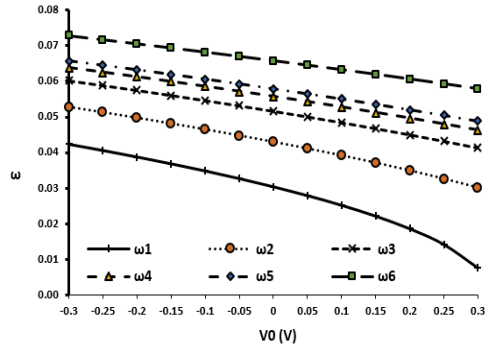

Fig. 7. The effect of the biaxial force V_0(V) on the dimensionless natural frequencies of the functionally graded piezoelectric nanoplate under trigonometric distribution of transverse shear deformation with $\lambda = 1$, $\mu = 0.4$ and $P_0 = 0$.

4. Conclusions

In this paper, free vibration of the functionally graded piezoelectric nanoplates based on exponential and trigonometric shear deformation theories using the nonlocal elasticity theory is investigated. Navier solution is applied to analysis the free vibration of the functionally graded piezoelectric nanoplates. Hamilton's principle is used to derive the governing equations of motion and associated boundary conditions. The material properties of functionally graded piezoelectric nanoplate are assumed to change through the thickness with a power law distribution. What presented herein illustrates the influences of the variations of the nonlocal parameter, gradient index, aspect ratio, length-to-thickness ratio, biaxial force and external electric voltage on the dimensionless natural frequencies values of a functionally graded piezoelectric nanoplate. From the comparison and discussion of numerical results, following conclusions can be deduced:

- The distribution of transverse shear stress is effective on the dynamic behavior of the structure so that neglecting the effects of transverse shear deformation will increase frequencies. The modified shear deformation theories utilized here do not require any shear correction factor and satisfy transverse shear traction free conditions on the top and the bottom surfaces of the functionally grade piezoelectric nanoplate.
- The nonlocal parameter has an important influence on natural frequencies of functionally graded piezoelectric nanoplate so that an increase in nonlocal parameter decreases the dimensionless natural frequencies.
- The dimensionless natural frequency decreases with increasing the gradient index of the nanoplate.
- The dimensionless fundamental natural frequency increases mildly in small amounts of aspect ratio and increases swiftly in larger quantities. Also, the size effect on the piezoelectric nanoplate has an increasingly strong trend with the increase of the aspect ratio.
- The dimensionless fundamental natural frequency reduces quickly with the raise of the length-to-thickness ratio and the size effect becomes less significant for the larger length-to-thickness ratio.
- The vibrational frequencies of functionally graded piezoelectric nanoplates are wholly responsive to the electro-mechanical loading, and they incline by applying tensile forces.

Acknowledgments

The authors gratefully acknowledge the funding by Arak University, under Grant No. 92/9834.

Nomenclature

l_a	Length of the plate
l_b	Width of the plate
h	Thickness of the plate
E	Young's modulus
υ	Poisson's ratio
ρ	Mass density

u_1	Displacement in the x_1 direction
u_2	Displacement in the x_2 direction
u_3	Displacement in the x_3 direction
σ_{ij}	Normal stresses
λ	Gradient index parameter
∇	Nabla operator
E_i	Electric field
D	Electric displacement
G	Shear modulus
ℓ	Material length scale parameter
Ω	Natural frequency of the nanoplate
P_0	Biaxial force
ε_{ij}	Normal strains
V_0	External electric voltage
Φ	Electric potential
I_i	Plate inertias

Appendix A

$$A_1 = \int_{-\frac{h}{2}}^{\frac{h}{2}} c_{11}\, dz,$$

$$A_{11} = \int_{-\frac{h}{2}}^{\frac{h}{2}} c_{11} z f_{(z)}\, dz, \quad \text{(A1-3)}$$

$$B_2 = \int_{-\frac{h}{2}}^{\frac{h}{2}} e_{31} \frac{2V_0}{h} dz,$$

$$A_2 = \int_{-\frac{h}{2}}^{\frac{h}{2}} c_{11} z\, dz, \quad \text{(A4-6)}$$

$$A_{12} = \int_{-\frac{h}{2}}^{\frac{h}{2}} c_{12} z^2\, dz,$$

$$B_3 = \int_{-\frac{h}{2}}^{\frac{h}{2}} e_{31} z\gamma \sin(\gamma z)\, dz,$$

$$A_3 = \int_{-\frac{h}{2}}^{\frac{h}{2}} c_{11} f_{(z)}\, dz, \quad \text{(A7-8)}$$

$$A_{13} = \int_{-\frac{h}{2}}^{\frac{h}{2}} c_{12} z f_{(z)}\, dz,$$

$$B_4 = \int_{-\frac{h}{2}}^{\frac{h}{2}} e_{31} z \frac{2V_0}{h} dz,$$

$$A_4 = \int_{-h/2}^{h/2} c_{12}\, dz, \quad \text{(A10-12)}$$

$$A_{14} = \int_{-\frac{h}{2}}^{\frac{h}{2}} c_{66} z^2\, dz,$$

$$B_5 = \int_{-\frac{h}{2}}^{\frac{h}{2}} e_{31} f_{(z)} \gamma \sin(\gamma z)\, dz,$$

$$A_5 = \int_{-\frac{h}{2}}^{\frac{h}{2}} c_{12} z\, dz, \quad \text{(A12-15)}$$

$$A_{15} = \int_{-\frac{h}{2}}^{\frac{h}{2}} c_{66} z f_{(z)}\, dz,$$

$$B_6 = \int_{-\frac{h}{2}}^{\frac{h}{2}} e_{31} f_{(z)} \frac{2V_0}{h} dz,$$

$$A_6 = \int_{-\frac{h}{2}}^{\frac{h}{2}} c_{12} f_{(z)}\, dz, \quad \text{(A15-18)}$$

$$A_{16} = \int_{-\frac{h}{2}}^{\frac{h}{2}} c_{11} {f_{(z)}}^2\, dz,$$

$$B_7 = \int_{-\frac{h}{2}}^{\frac{h}{2}} e_{15} \frac{\partial f_{(z)}}{\partial z} \cos(\gamma z)\, dz,$$

$$A_7 = \int_{-h/2}^{h/2} c_{66}\, dz, \quad \text{(A18-21)}$$

$$A_{17} = \int_{-\frac{h}{2}}^{\frac{h}{2}} c_{12} {f_{(z)}}^2\, dz,$$

$$B_8 = \int_{-\frac{h}{2}}^{\frac{h}{2}} d_{11} (\cos(\gamma z))^2\, dz,$$

$$A_8 = \int_{-\frac{h}{2}}^{\frac{h}{2}} c_{66} z\, dz, \quad \text{(A22-24)}$$

$$A_{18} = \int_{-h/2}^{h/2} c_{66} {f_{(z)}}^2\, dz,$$

$$B_9 = \int_{-\frac{h}{2}}^{\frac{h}{2}} d_{33} (\gamma \sin(\gamma z))^2\, dz,$$

$$A_9 = \int_{-\frac{h}{2}}^{\frac{h}{2}} c_{66} f_{(z)}\, dz, \quad \text{(A25-27)}$$

$$A_{19} = \int_{-\frac{h}{2}}^{\frac{h}{2}} c_{44} \left(\frac{\partial f_{(z)}}{\partial z}\right)^2 dz,$$

$$B_{10} = \int_{-\frac{h}{2}}^{\frac{h}{2}} d_{33} \gamma \sin(\gamma z) \frac{2V_0}{h} dz,$$

$$A_{10} = \int_{-\frac{h}{2}}^{\frac{h}{2}} c_{11} z^2\, dz, \quad \text{(A28, 29)}$$

$$B_1 = \int_{-\frac{h}{2}}^{\frac{h}{2}} e_{31} \gamma \sin(\gamma z)\, dz,$$

References

[1] Li, Y., Cheng, L. and Li, P., 2003. Modeling and vibration control of a plate coupled with piezoelectric material. *Composite Structures,* 62(2), pp.155-162.

[2] Khorshidi, K., Rezaei, E., Ghadimi, A. and Pagoli, M., 2015. Active vibration control of circular plates coupled with piezoelectric layers excited by plane sound wave. *Applied Mathematical Modelling,* 39(3-4), pp.1217-1228.

[3] Eringen, A.C., 2002. *Nonlocal continuum field theories*: Springer Science & Business Media.

[4] Mindlin, R. and Tiersten, H., 1962. Effects of couple-stresses in linear elasticity. *Archive for Rational Mechanics and Analysis,* 11(1), pp.415-448.

[5] Fleck, N. and Hutchinson, J., 1993. A phenomenological theory for strain gradient effects in plasticity. *Journal of the Mechanics and Physics of Solids,* 41(12), pp.1825-1857.

[6] Chen, C., Shi, Y., Zhang, Y. S., Zhu, J. and Yan, Y., 2006. Size dependence of Young's modulus in ZnO nanowires. *Physical Review Letters,* 96(7), pp.075505.

[7] Stan, G., Ciobanu, C., Parthangal, P. M. and Cook, R. F., 2007. Diameter-dependent radial and tangential elastic moduli of ZnO nanowires. *Nano Letters,* 7(12), pp.3691-3697.

[8] Khorshidi, K. and Fallah, A., 2017. Effect of Exponential Stress Resultant on Buckling Response of Functionally Graded Rectangular Plates. *Journal of Stress Analysis,* 2(1), pp.27-33.

[9] Khorshidi, K. and Karimi, M., 2019. Analytical modeling for vibrating piezoelectric nanoplates in interaction with inviscid fluid using various

modified plate theories. *Ocean Engineering,* 181, pp. 267-280.
[10] Meskini, M. and Ghasemi, A. R., 2020. Electro-magnetic potential effects on free vibration of rotating circular cylindrical shells of functionally graded materials with laminated composite core and piezo electro-magnetic two face sheets. *Journal of Sandwich Structures and Materials,* DOI: 10.1177/1099636220909751.
[11] Khorshidi, K. and Karimi, M., 2019. Analytical approach for thermo-electro-mechanical vibration of piezoelectric nanoplates resting on elastic foundations based on nonlocal theory. *Mechanics of Advanced Composite Structures,* 6(2), pp.117-129.
[12] Ghasemi, A., Taheri-Behrooz, F., Farahani, S. and Mohandes, M., 2016. Nonlinear free vibration of an Euler-Bernoulli composite beam undergoing finite strain subjected to different boundary conditions. *Journal of Vibration and Control,* 22(3), pp.799-811.
[13] Mohandes, M., Ghasemi, A. R., Irani-Rahagi, M., Torabi, K. and Taheri-Behrooz, F., 2018. Development of beam modal function for free vibration analysis of FML circular cylindrical shells. *Journal of Vibration and Control,* 24(14), pp.3026-3035.
[14] Norouzzadeh, A., Ansari, R. and Rouhi, H., 2018. Isogeometric vibration analysis of small-scale Timoshenko beams based on the most comprehensive size-dependent theory. *Scientia Iranica, Transaction F: Nanotechnology*, 25(3), pp.1864-1878.
[15] Ansari, R. and Gholami, R., 2016. Nonlocal nonlinear first-order shear deformable beam model for post-buckling analysis of magneto-electro-thermo-elastic nanobeams. *Scientia Iranica, Transaction F: Nanotechnology,* 23(6), pp.3099-3114.
[16] Ebrahimi, F. and Barati, M. R., 2017. Hygrothermal effects on vibration characteristics of viscoelastic FG nanobeams based on nonlocal strain gradient theory. *Composite Structures,* 159, pp.433-444.
[17] Liu, C., Ke, L.L., Wang, Y.S., Yang, J. and Kitipornchai, S. 2013. Thermo-electro-mechanical vibration of piezoelectric nanoplates based on the nonlocal theory. *Composite Structures,* 106**,** pp.167-174.
[18] Ke, L.L., Liu, C. and Wang, Y.S., 2015. Free vibration of nonlocal piezoelectric nanoplates under various boundary conditions. *Physica E: Low-dimensional Systems and Nanostructures*, 66, pp.93-106.
[19] Wang, K. and Wang, B., 2012. The electromechanical coupling behavior of piezoelectric nanowires: surface and small-scale effects. *Europhysics Letters,* 97(6), 66005.
[20] Khorshidi, K. and Karimi, M., 2020. Fluid-structure interaction of vibrating composite piezoelectric plates using exponential shear deformation theory. *Mechanics of Advanced Composite Structures,* 7(1), pp.59-69.
[21] Jabbarian, S. and Ahmadian, M., 2018. Free vibration analysis of functionally graded stiffened micro-cylinder based on the modified couple stress theory. *Scientia Iranica, Transaction B: Mechanical Engineering,* 25(5), pp.2598-2615.
[22] Fatan, A. and Ahmadian, M., 2018. Vibration analysis of FGM rings using a newly designed cylindrical superelement. *Scientia Iranica, Transaction B: Mechanical Engineering,* 25(3), pp.1179-1188.
[23] Karimi, M., Khorshidi, K., Dimitri, R. and Tornabene, F., 2020. Size-dependent hydroelastic vibration of FG microplates partially in contact with a fluid. *Composite Structures,* 244, 112320.
[24] Shahmohamadi, M. and Kabir, M., 2017. Effects of shear deformation on mechanical and thermo-mechanical nonlinear stability of FGM shallow spherical shells subjected to uniform external pressure. *Scientia Iranica, Transaction A: Civil Engineering,* 24(2), pp.584-596.
[25] Bayat, A., Moosavi, H. and Bayat, Y., 2015. Thermo-mechanical analysis of functionally graded thick spheres with linearly time-dependent temperature. *Scientia Iranica. Transaction B: Mechanical Engineering,* 22(5)**,** pp.1801.
[26] Ghasemi, A., Kazemian, A. and Moradi, M., 2014. Analytical and numerical investigation of FGM pressure vessel reinforced by laminated composite materials. *Journal of Solid Mechanics*, 6(1), pp.43-53.
[27] Wu, C.P. and Tsai, T.C., 2012. Exact solutions of functionally graded piezoelectric material sandwich cylinders by a modified Pagano method. *Applied Mathematical Modelling,* 36(5), pp.1910-1930.
[28] Khorshidi, K., Bahrami, M., Karimi, M. and Ghasemi, M., 2020. A theoretical approach for flexural behavior of FG vibrating micro-plates with piezoelectric layers considering a hybrid length scale parameter. *Journal of Theoretical and Applied Vibration and Acoustics,* 6(1), pp.51-68.
[29] Khorshidi, K. and Karimi, M., 2019. Flutter analysis of sandwich plates with functionally graded face sheets in thermal environment. *Aerospace Science and Technology,* 95, 105461.
[30] Ghugal, Y. and George, J.T., 2010. Free vibration of thick isotropic plates using trigonometric shear deformation theory. *Advances and Trends in Structural Engineering, Mechanics and Computation,* 3(2), pp.172-182.
[31] Sayyad, A. S. and Ghugal, Y. M., 2012. Bending and free vibration analysis of thick isotropic plates by using exponential shear deformation theory. *Applied and Computational Mechanics,* 6(1), pp.65-82.

[32] Ghugal, Y.M. and Sayyad, A.S., 2011. Free vibration of thick orthotropic plates using trigonometric shear deformation theory. *Latin American Journal of Solids and Structures,* 8(3), pp.229-243.
[33] Ferreira, A., Roque, C. and Jorge, R., 2005. Analysis of composite plates by trigonometric shear deformation theory and multiquadrics. *Computers and Structures,* 83(27), pp.2225-2237.
[34] Zenkour, A.M., 2006. Generalized shear deformation theory for bending analysis of functionally graded plates. *Applied Mathematical Modelling,* 30(1), pp.67-84.
[35] Ghugal, Y.M. and Sayyad, A.S., 2013. Stress analysis of thick laminated plates using trigonometric shear deformation theory. *International Journal of Applied Mechanics,* 5(1), 1350003.
[36] Khorshidi, K., Karimi, M. and Amabili, M., 2020. Aeroelastic analysis of rectangular plates coupled to sloshing fluid. *Acta Mechanica,* 231(8), pp.3183-3198.
[37] Mantari, J. and Soares, C.G., 2014. A trigonometric plate theory with 5-unknowns and stretching effect for advanced composite plates. *Composite Structures,* 107, pp.396-405.
[38] Rango, R.F., Nallim, L.G. and Oller, S., 2015. Formulation of enriched macro elements using trigonometric shear deformation theory for free vibration analysis of symmetric laminated composite plate assemblies. *Composite Structures,* 119, pp.38-49.
[39] Khorshidi, K. and Fallah, A., 2016. Buckling analysis of functionally graded rectangular nano-plate based on nonlocal exponential shear deformation theory. *International Journal of Mechanical Sciences,* 113, pp. 94-104.
[40] Wang, Y., Xu, R. and Ding, H., 2010. Analytical solutions of functionally graded piezoelectric circular plates subjected to axisymmetric loads. *Acta Mechanica,* 215(1-4), pp.287-305.
[41] Chen, W. and Ding, H., 2002. On free vibration of a functionally graded piezoelectric rectangular plate. *Acta Mechanica,* 153(3-4), pp.207-216.
[42] Ueda, S., 2008. A cracked functionally graded piezoelectric material strip under transient thermal loading. *Acta Mechanica,* 199(1-4), pp.53-70.
[43] Khorshidi, K., Ghasemi, M., Karimi, M. and Bahrami, M., 2019. Effects of couple-stress resultants on thermo-electro-mechanical behavior of vibrating piezoelectric micro-plates resting on orthotropic foundation. *Journal of Stress Analysis,* 4(1), pp.125-136.
[44] Murmu, T. and Adhikari, S., 2010. Nonlocal effects in the longitudinal vibration of double-nanorod systems. *Physica E: Low-dimensional Systems and Nanostructures,* 43(1), pp.415-422.
[45] Roostai, H. and Haghpanahi, M., 2014. Vibration of nanobeams of different boundary conditions with multiple cracks based on nonlocal elasticity theory. *Applied Mathematical Modelling,* 38(3), pp.1159-1169.
[46] Wang, Q., 2002. Axi-symmetric wave propagation in a cylinder coated with a piezoelectric layer. *International Journal of Solids and Structures,* 39(11), pp.3023-3037.
[47] Bodaghi, M. and Shakeri, M., 2012. An analytical approach for free vibration and transient response of functionally graded piezoelectric cylindrical panels subjected to impulsive loads. *Composite Structures,* 94(5), pp.1721-1735.